Detection of cavities in an urban environment: Case of M'Rara region (Northeast of Algeria)

Boualem Bouyahiaoui[1 #], Abdeslam Abtout[1]

[1]Center of Research in Astronomy, Astrophysics and Geophysics, Route de l'Observatoire, Bouzaréah, 16340 Alger, Algeria.

[#]Corresponding author: b.bouyahiaoui@yahoo.com

ABSTRACT

Micro-gravimetry emerges as the most appropriate geophysical technique for cavity detection in urban or industrial settings, as it remains unaffected by surrounding electromagnetic influences. The presented study investigates the occurrence of fissures, land subsidence, collapse events, and their potential association with the formation of cavities at depth. These phenomena were observed near a sealed hydraulic drilling site located in the M'Rara area within the Northeast Algerian Sahara basin. This drilling operation was sealed off due to the inflow of saline water, with a salt layer identified at a depth of 936 m according to the stratigraphic column. A gravimetric survey was conducted to image the lateral and vertical density variation. The resulting gravimetric image allows in comprehending the observed geological phenomena and their potential correlation with the presence of cavities at the salt layer.

Keywords: Gravity survey, collapse, land subsidence, fissure.

1. Introduction

The M'Rara region lies within the Northeast Algerian Sahara basin, a region prone to various natural hazards, as indicated by Foudili et al. (2019). In 1960, hydraulic drilling was conducted to tap into the Albian aquifer and provide the town of M'Rara with water for drinking and irrigation purposes (Fig. 1). The stratigraphic analysis uncovered a salt layer measuring 11 meters thick, situated at depths ranging from 947 to 936 meters. Ten years into operation, during the 1970s, the drilling commenced pumping 1200 l/mn of saline water with a concentration of 315 g/l. Subsequently, the drilling was sealed with a cement plug. Near to this drilling site, there is a fenced building utilized as a cooling system for the hot water emanating from the Albian aquifer. Within this structure, a circular depression with a diameter of 5 meters indicates the possible presence of cavity below. At 117 m, to the northeast of this hydraulic drilling site, a collapse appeared. To the northwest of the hydraulic drilling site, at 1.3 km to the first collapse a second collapse manifested (Fig. 2a). Furthermore, alongside these collapses and land subsidence events, a significant fissure is present in the Plio-quaternary agglomerates, located 770 meters southwest of the hydraulic drilling site.

We seek to comprehend the correlation with the potential presence of a cavity within the salt layer. To accomplish this goal, we carried out a gravimetric survey in the M'Rara region to visualize the density distribution and interpret anomalous areas in correlation with the potential presence of cavities.

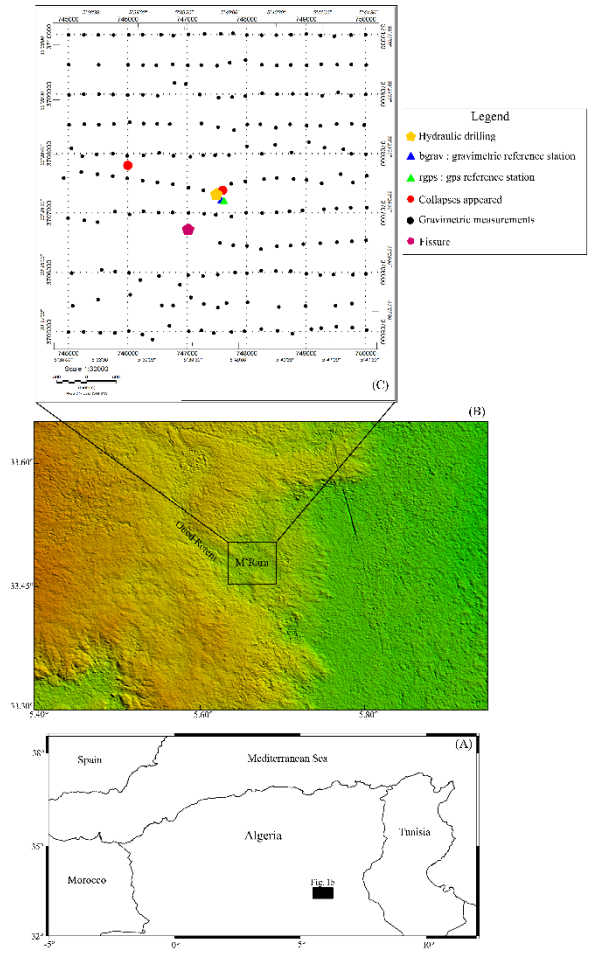

Figure 1. (a) North Algeria location map. (b) Location map of the studied area superimposed on the topographic relief map from ETOPO1 1-min global relief in m (www.ngdc.noaa.gov). (c) gravimetric dataset collected in this study.

2. Geological setting

The M'Rara region comprises a rural settlement surrounded by agricultural fields. Characterized by a Saharan-type arid climate, it experiences hot, dry summers and milder winters. Situated in a Plio-quaternary basin at approximately 100 meters altitude, it spans an area of approximately 15 km², surrounded by Mio-Pliocene hills (Fig. 2b). It falls within the Saharan platform domain, which underwent structural changes during the Upper Paleozoic, forming several basins divided by shoals (Ballais, 2010). The region remained relatively stable during the Meso-Cenozoic period, except for compressive events during the late Aptian (lower Cretaceous), resulting in N-S oriented anticlines, and further compressive phases during the Cenozoic.

The M'Rara area hosts two significant aquifer systems. The first system is the complex terminal (CT), characterized by two primary aquifers separated by semi-impermeable to impermeable layers (Fig. 2c). Above lies the shallow aquifer situated within the Mio-Pliocene sands, while below is the aquifer located within the late Eocene and early Senonian carbonate limestone (Guendouz et al., 2003).

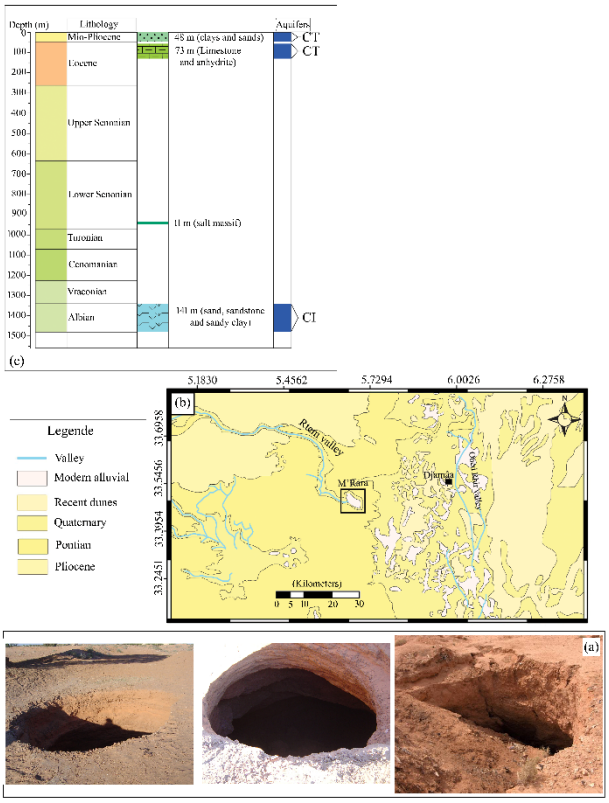

Figure 2. (a) Surface observation. (b) The geological map around the M'Rara region. (c) The lithostratigraphic column within the hydraulic borehole, positioned at the center of M'Rara town.

3. Gravimetric maps

The gravimetric results or the gravimetric anomalies are images of masses distribution in the basement (Oldham and Sutherland, 1955; Blakely, 1995; Bouyahiaoui et al., 2017; Hackney, 2020; Bendali et al., 2019; Bayou et al., 2023). These images don't directly reflect the presence of masses or voids, but the apparent variation of density which is created by this mass or void. Therefore, by analysis of this density distribution, we will attribute their origins, such as cavities, decompressions, geological accidents (Baranov 1953; Oldham and Sutherland, 1955; Bhattacharyya and Chan, 1977; Thompson, 1982; Gibert and Galdeano, 1985; Reid et al., 1990; Mikhailov et al., 2003; Abtout et al., 2014; Bendali et al., 2022; Bouyahiaoui et al., 2024).

The gravimetric measurements were acquired using a terrestrial Scintrex CG3 gravimeter. A total of 225 gravity measurements distributed almost regularly manner along square grid of 5*5 km² (black circles, Fig. 1c). The hydraulic drilling represents the centre of this grid. This measurements grid is composed by 11 East-west profiles, with a length of 5 km and spaced by 500 m. Each profile is composed by 20 gravimetric stations, spaced by 250 m. the density of measurements is about of 15 gravimetric measurements per km².

The main document for interpreting gravimetric data is the complete Bouguer gravity anomaly. It represents the difference between gravity measured and a model value at the same point that is based on the normal gravity of a reference ellipsoid, corrected for the gravity effects of elevation above the reference ellipsoid and the mass of rock between the point and the reference ellipsoid (Hackney, 2020). So, the complete Bouguer anomaly values are given following relationship (1):

$$g_b = g_{mes} - g(\varphi) + (0.3086\, h_s) - (0.0419\, d.h_s) + g_T \quad (1)$$

Where g_{mes} is the station measured gravity, $g(\varphi)$ represents the theoretical gravity calculated within the IUGG1967 system, h_s is the station elevation, d represents the density correction and g_T is the topographic correction. The data was uniformly reduced with a density of 2400 kg/m^3 for the Bouguer correction.

The Bouguer anomaly map is drawn from a regular grid of the Bouguer anomaly values. It is obtained by interpolation using the minimum curvature method, with equidistance contour lines of 0.05 mGal (Fig. 3). The Bouguer anomaly values are ranging from -55.590 to -54.400 mGal. This map shows three big anomalies, two with highs values and a third characterized by low values. The first high anomaly (A1) is located at the North. Its shape is quasi-circular and presents Bouguer anomaly values of about of -54.570 mGal. The second high anomaly (A2) is situated at the South. It is about of a set of high anomalies, with north-south orientation. The Bouguer anomaly value of this high set is about of -54.400 mGal. The (A1) and (A2) high anomalies seem to be connected by an N-S positive axis. These two positive anomalies correspond to the Miocene. The third big anomaly (A3), with low values, is located at the North-East. These Bouguer anomaly values are about of -55.514 mGal. It corresponds to Quaternary continental. In addition of these variations of long wavelengths, a several circular anomalies of short wavelengths are observed.

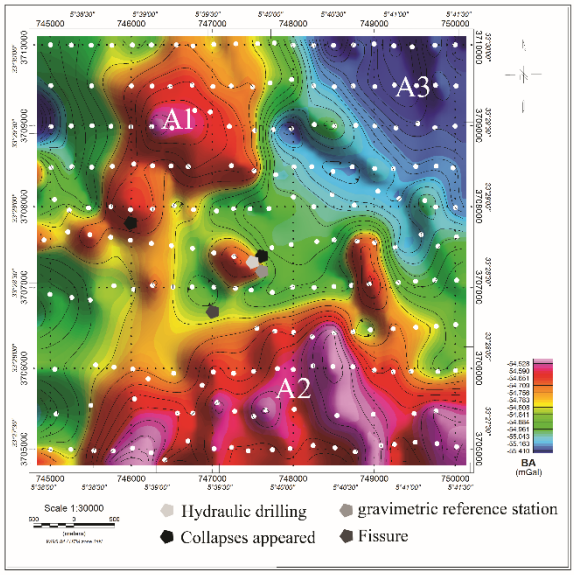

Figure 3. The Bouguer anomaly (BA) of the M'Rara area. The data were uniformly reduced with a density of 2400 kg/m^3 for the Bouguer correction.

The Bouguer anomaly map shown in Figure 3 is integral, it includes the sum of different effects: superficial, deep and intermediate. So, it is necessary to separate all these effects. To remove the regional effect and isolate solely the local (residual) anomalies, we implement the polynomial method at various orders. (Oldham and Sutherland, 1955; Mickus et al., 1991; Bendali et al., 2022; Bayou et al., 2023; Bouyahiaoui et al., 2024). This technique approaches the measured field by a polynomial in x and in y. The different order will be chosen according to the favourite pattern which represents the regional. We have removed polynomials of different orders (1, 2 and 3) from measures, following equation (2):

$$P(x,y) = \sum_{i=0}^{n} a_i U_i(x,y) \qquad (2)$$

Where $U_i(x,y)$ basic function corresponds to the product of two orthogonal polynomials and a_i represents the real coefficients of the polynomial.

The residual map represents anomalies values ranging between -0.328 and +0.468 mGal. We notice two distinguished areas. Highs values with positives anomalies at the East and at the north, whereas the western part is characterized by low values and negatives anomalies (Fig. 4). Along the residual map collapses, land subsidence and fissure are located within negatives anomalies. Theses negatives anomalies reflect the presence in the subsoil of low-density masses to zero density (case of cavities). While positive anomalies are clue of the presence of heavy masses (dense). As the aim of our study is detection of possible cavities, we will be interested, only, in negative anomalies (Ano1 to Ano4, Fig. 4).

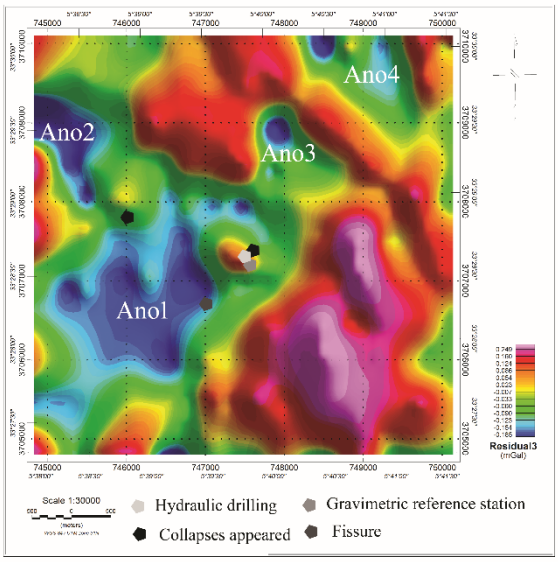

Figure 4. The residual map obtained by subtracting a polynomial of order 3.

4. Discussion

The gradients filter (vertical and horizontal) accentuates gravity lineaments indicative of faults or boundaries between geological structures. The horizontal gradient filter is one of the techniques employed to identify the horizontal boundaries of the gravity causative sources (Blakely, 1995; Jacoby and Smilde., 2009). The gradient map associated with it facilitates the identification of density variations across the horizontal plane (Fig. 5). The vertical gradient (Fig. 6) allows recognizing local and shallow features (Baranov, 1953; Aydogan, 2011). Along the horizontal and vertical gradients maps a series of NW-SE lineaments is observed on almost all the study area. This alignment coincides with the Oued Retem valley (see position in Fig. 1b) and flow direction of Mio-Pliocene shallow water table. Tectonic deformation exists in the Miocene, they express the backlash of the tectonic events in relation with the creation, in the Cenozoic, of the Atlas domain. They are reflected mainly on the outcrop scale, by joints almost perpendicular to the stratification. Some of them are filled with amorphous calcite.

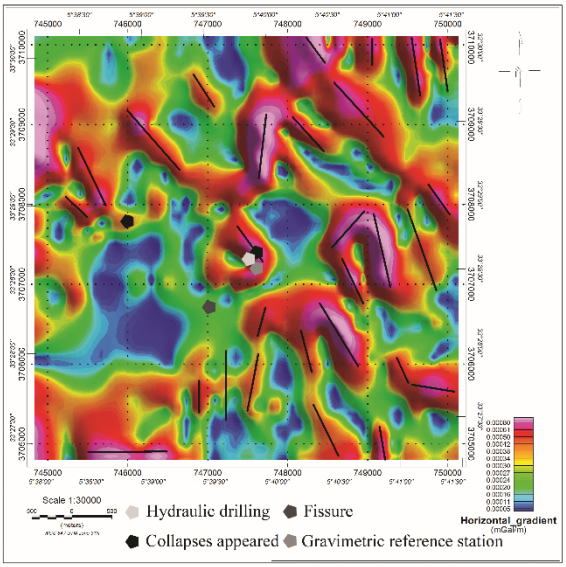

Figure 5. The horizontal gradient (HG) map of the Bouguer anomaly.

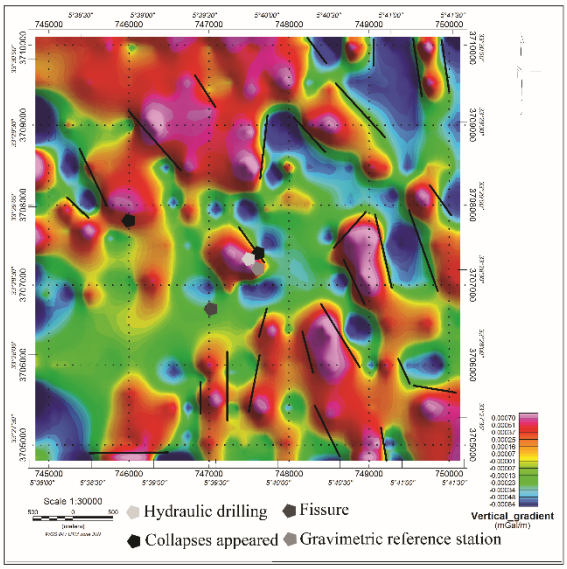

Figure 6. The vertical gradient (VG) map of the Bouguer anomaly.

5. Conclusion

Geological surface observations indicate no evidence suggesting a potential large-scale collapse in the vicinity of the M'Rara hydraulic drilling site. Furthermore, gravity data at the salt layer, approximately 1000 meters deep, reveals no anomalies beneath this drilling location. While dismissing the involvement of hydraulic drilling in the creation of fissures and collapses, this study underscores a significant risk facing the area due to the presence of shallow cavities. These cavities are believed to form as a result of water circulation in the subsoil originating from the Retem valley. A phenomenon accentuated by the more permanent character of the waters of the Albian, brought by the various boreholes and mainly used for the irrigation of crops. Indeed, the collapses and subsidence observed on the surface appear to be organized at the borders of dense and consolidated bodies associated probably to the limestone, which form a barrier against the circulation of underground water at shallow depths. Thus, the water being channelled, hits the less consolidated formations which undergo strong erosion, their materials are then transported elsewhere.

Acknowledgements

The field campaign was carried out by CRAAG (Centre de Recherche en Astronomie, Astrophysique et Géophysique – Observatoire d'Alger). The authors would like to express their gratitude for the financial support received during this study.

References

Abtout, A., Boukerbout, H., Bouyahiaoui, B., & Gibert, D., 2014. Gravimetric evidences of active faults and underground structure of the Cheliff seismogenic basin (Algeria). Journal of African Earth Sciences. 99, 363–373. http://doi.org/10.1016/j.jafrearsci.2014.02.011

Aydogan, D. (2011). Extraction of lineaments from gravity anomaly maps using the gradient calculation: Application to Central Anatolia. Earth Planet Sp 63, 903–913. https://doi.org/10.5047/eps.2011.04.003

Ballais, J. L, 2010, Des oueds mythiques aux rivières artificielles : l'hydrographie du Bas-Sahara algérien. Physio-Géo. Géographie Physique et Environnement. 4, 107–127. https://doi.org/10.4000/physio-geo.1173

Baranov, V., 1953, Calcul du gradient vertical du champ de gravité ou du champ magnétique mesuré à la surface du sol. Earth Sciences, Geophysical Prospecting, 1, 171–191. https://doi.org/10.1111/j.1365-2478.1953.tb01139.x

Bayou, Y., Abtout, RA., Renaut, R.A., Bouyahiaoui, B., Maouche, S., Vatankhah, S., Berguig, M.C., 2023. The northeastern Algeria hydrothermal system: gravimetric data and structural implication. Geotherm Energy 11, 14. https://doi.org/10.1186/s40517-023-00258-2

Bendali, M., Bouyahiaoui, B., Boukerbout, H., Nèche, B., Bentridi, S. E., Abtout, A. (2019). Gravimetric study of the Khemis Miliana plain (upper Cheliff basin): Structure of the transition zone between the Cheliff and Mitidja basin (North of Algeria). In: Rossetti, F. Et al. (eds.), The Structural Geology Contribution to the Africa-Eurasia Geology: Basement and Reservoir Structure, Ore Mineralisation and Tectonic Modelling. CAJG 2018. Advances in Science, Technology & Innovation (IEREK Interdisciplinary Series for Sustainable Development). Springer, Cham. https://doi.org/10.1007/978-3-030-01455-1_60

Bendali, M., Abtout, A., Bouyahiaoui, B., Boukerbout, H., Marok, A., and Reolid, M., 2022. Interpretation of new gravity survey in the seismogenic Upper Chelif Basin (North of Algeria): Deep structure and modeling. Journal of Iberian Geology, 48, 205–224. https://doi.org/10.1007/s41513-022-00190-7

Bhattacharyya, B. K. and Chan, K. C., 1977, Reduction of magnetic and gravity data on an arbitrary surface acquired in a region of high topographic relief. Geophysics, 42, 1411–1430.

Blakely, R. J. 1995, Potential theory in gravity and magnetic applications. Cambridge University Press, Cambridge (UK). https://doi.org/10.1017/CBO9780511549816

Bouyahiaoui, B., Abtout, A., Hamai, L., Boukerbout, H., Djellit, H., Bougchiche, S., Bendali, M., & Bouabdallah, H., 2017. Structural architecture of the hydrothermal system from geophysical data in Hammam Bouhadjar area (northwest of Algeria). Pure and Applied Geophysics, 174, 1471–1488. https://doi.org/10.1007/s00024-017-1479-0

Bouyahiaoui, B., Boukerbout, H., Bendali, M., Bayou, Y & Abtout, A., 2024. Mining Potential of the Upper Cheliff Area (North of Algeria): Gravimetric and Magnetic Evidences. Pure and Applied Geophysics. https://doi.org/10.1007/s00024-023-03424-6

Foudili, D., Bouzid, A., Berguig, M. C., Bougchiche, S. S., Abtout, A., and Guemache, M. A., 2019. Investigating karst collapse geohazards using magnetotellurics: A case study of M'rara basin, Algerian Sahara. Journal of Applied Geophysics, 160, 144–156. https://doi.org/10.1016/j.jappgeo.2018.11.011

Jacoby, W., and P.L. Smilde., 2009, Gravity interpretation. Fundamentals and application of gravity inversion and geological interpretation. Springer–Verlag Berlin Heidelberg, 413 p. ISBN 978-3-540-85329-9.

Gibert, D. and Galdeano, A. 1985, A computer program to perform transformations of gravimetric and aeromagnetic survey. Computers & Geoscience, 11, 553–588.

Guendouz, A., Moulla, A. S., Edmunds, W. M., Zouari, K., Shand, P., Mamou, A., 2003, Hydrogeochemical and isotopic evolution of water in the complexe terminal aquifer in the Algerian Sahara. Hydrogeology Journal, 11, 483–495. https://doi.org/10.1007/s10040-003-0263-7

Hackney, R., 2020, Gravity, data to anomalies. In: Gupta H. (eds) Encyclopedia of Solid Earth Geophysics. Encyclopedia of Earth Sciences Series. Springer, Cham. https://doi.org/10.1007/978-3-030-10475-7_78-1

Mikhailov, V., Galdeano, A., Diament, M., Gvishiani, A., Agayan, S., Bogoutdinov, S., Graeva, E., and Sailhac, P., 2003, Application of artificial intelligence for Euler solutions clustering. Geophysics, 68, 168–180, https://doi.org/10.1190/1.1543204

Mickus, K.L., Aiken, C. L.V., & Kennedy, W.D. (1991). Regional-residual gravity anomaly separation using the minimum-curvature technique, Geophysics, Vol. 56, NO.2, 279–283, https://doi.org/10.1190/1.1443041

Oldham, C. W. and Sutherland, D. B., 1955, Orthogonal polynomials: their use in estimating the regional effect. Geophysics, 20, 295–306.

Reid, A. B., Allsop, J. M., Granser, H., Millett, A. J., and Somerton, I. W., 1990, Magnetic interpretation in three dimensions using Euler deconvolution. Geophysics, 55, 80–91.

Thompson, D. T, 1982, EULDPH: A new technique for making computer-assisted depth estimates from magnetic data. Geophysics, 47, 31–37.